

Cervical Spine Disc Deformation During *In Vivo* Three-Dimensional Head Movements

WILLIAM ANDERST, WILLIAM DONALDSON, JOON LEE, and JAMES KANG

Department of Orthopaedic Surgery, Biodynamics Lab, University of Pittsburgh, 3820 South Water Street, Pittsburgh, PA 15203, USA

(Received 14 May 2015; accepted 7 August 2015; published online 14 August 2015)

Associate Editor Joel D. Stitzel oversaw the review of this article.

Abstract—Although substantial research demonstrates that intervertebral disc cells respond to mechanical signals, little research has been done to characterize the *in vivo* mechanical environment in the disc tissue. The objective of this study was to estimate cervical disc strain during three-dimensional head movements. Twenty-nine young healthy adults performed full range of motion flexion/extension, lateral bending, and axial rotation of the head within a biplane radiography system. Three-dimensional vertebral kinematics were determined using a validated model-based tracking technique. A computational model used these kinematics to estimate subject-specific intervertebral disc deformation (C3–4 to C6–7). Peak compression, distraction and shear strains were calculated for each movement, disc level, and disc region. Peak compression strain and peak shear strain were highest during flexion/extension (mean \pm 95% confidence interval) (32 ± 3 and $86 \pm 8\%$, respectively), while peak distraction strain was highest during lateral bending ($57 \pm 5\%$). Peak compression strain occurred at C4–5 ($33 \pm 4\%$), while peak distraction and shear strain occurred at C3–4 (54 ± 8 and $83 \pm 11\%$, respectively). Peak compression, distraction, and shear strains all occurred in the posterior–lateral annulus (48 ± 4 , 80 ± 8 , and $109 \pm 12\%$, respectively). These peak strain values may serve as boundary conditions for *in vitro* loading paradigms that aim to assess the biologic response to physiologic disc deformations.

Keywords—Disc strain, Disc mechanobiology, Disc degeneration, Spine loading, Spine kinematics.

INTRODUCTION

A recent survey estimated that 13.6 million adults in the United States sought medical care for a primary diagnosis of a spine condition in 2008. The total cost to

care for these individuals was approximately \$13 billion.¹¹ Spine-related pain and dysfunction is believed to be initiated by intervertebral disc degeneration.²² The development and progression of intervertebral disc degeneration is influenced by the complex interactions between cells, extracellular matrix, and mechanical loading.³⁶ These interactions between mechanical loading and the biology of the disc (i.e., “mechanobiology”) determine whether the disc tissue remains in homeostasis, accumulates damage, or otherwise remodels in response to loading conditions.¹⁹

Although substantial research demonstrates that cells respond to mechanical signals,^{10,33} it is unclear which mechanical signals affect the cells most: stress, or strain.¹ In either case, the precise mechanical stimuli experienced by cells during *in vivo* loading remain poorly defined³³ because little research has been done to characterize the *in vivo* mechanical environment in the disc tissue.^{27,29,32,37} This is unfortunate, because applying the wrong type or magnitude of loading to tissue explants will lead to very different cell responses, and potentially misleading results.¹

A few studies have characterized the *in vivo* mechanical environment of the disc by inserting a pressure transducer into the discs of live volunteers.^{16,30,37} Although these studies reported disc pressures in static positions and while performing various activities, the results must be interpreted with caution due to the small number of volunteers and the inability of the pressure sensor to characterize disc mechanics over the entire volume of the disc simultaneously. A less invasive and more comprehensive alternative to this technique is to employ a computational model to characterize the disc mechanical environment.

Address correspondence to William Anderst, Department of Orthopaedic Surgery, Biodynamics Lab, University of Pittsburgh, 3820 South Water Street, Pittsburgh, PA 15203, USA. Electronic mail: anderst@pitt.edu

Therefore, the objective of this study was to develop a computational model to estimate disc strain in the cervical spine during three-dimensional head movements. It was hypothesized that: (1) Disc strains are higher during flexion/extension than during the combined motion that occurs during bending and rotation (*The Effect of Movement*), (2) Disc strains are greatest at the C5–6 and C6–7 discs and smallest at the C3–4 and C4–5 disc (*The Effect of Disc Level*), and (3) Disc strains are higher in the posterior–lateral annulus than in all other disc regions (*The Effect of Disc Region*).

MATERIALS AND METHODS

Subjects

Following Institutional Review Board (IRB) approval, data was collected from 29 subjects (15 M: average age 26.4 ± 3.9 years, age range 20–31, 14 F: average age 28.2 ± 4.9 years; age range 20–35) who provided informed consent to participate in this study. All participants were healthy asymptomatic non-smokers, with no history of neck surgery, chronic neck pain or diagnosis of osteoporosis, between the ages of 20 and 35. All participants were capable of performing full range of motion head and neck movements without limitations or pain. Pregnant women and individuals with any current or previous injury or disease that interferes with spine function were excluded. Recruitment was accomplished through on-campus flyers, an advertisement in an employee newsletter, and word of mouth.

Data Collection

Participants were seated upright within a custom designed biplane X-ray system³⁵ and directed to hold still and look straight ahead. Biplane radiographs of the cervical spine were collected for 0.1 s for a “static neutral” trial. Next, a total of 9 dynamic, full range of motion (ROM) movement trials were collected for each participant (three each of flexion/extension, lateral bending, and axial rotation). For each dynamic movement trial, participants were instructed to move their head and neck through their full range motion in a continuous fashion. A metronome set at 40–44 beats per minute was used to assist the participants in moving at a continuous, steady pace and complete each full movement cycle in approximately 3 s. As the subject performed 5–10 continuous cycles of the full ROM movement, one complete cycle of motion was captured by biplane radiographs, collected at 30 frames per second for 3.2 s (X-ray parameters: 70 kV, 160 mA, 2.5 ms X-ray pulses, source-to-subject dis-

tance 140 cm). Data was collected in this way for each dynamic movement trial, with a brief rest period between trials. For each participant, two of the three trials for each dynamic movement (selected by radiographic image quality) were included in the analysis. Additionally, four reflective markers placed on the head (the left and right Zygomatic arch, middle of the forehead, and the chin) and four reflective markers placed on the torso (left and right Acromion process, spinous process of C7, and sternum) were tracked at 60 Hz to determine global head ROM during each trial using a conventional optical motion analysis system (Vicon MX, Centennial, CO, USA).

Next, high-resolution CT scans ($0.29 \times 0.29 \times 1.25$ mm voxels) of the cervical spine (C1–T1) were acquired from each participant (GE Lightspeed 16, GE Medical Systems Inc., Waukesha, WI, USA). The effective radiation dose for each dynamic motion trial was estimated to be 0.16 mSv (determined using PCXMC simulation software, STUK, Helsinki, Finland). Therefore, the total radiation exposure associated with the biplane radiograph testing was approximately 1.5 mSv. The effective dose of a cervical spine CT scan has been reported to be between 3.0 and 4.36 mSv.^{8,12}

Data Processing

Bone tissue was segmented from the CT volume to generate a three-dimensional (3D) model of each vertebra (Simpleware software, Exeter, UK). Markers were interactively placed on the 3D bone models to define bone-specific anatomic coordinate systems.³¹ *In vivo* bone motion was tracked using a volumetric model-based tracking technique previously described in detail.^{3,6,7} This model-based tracking technique has been validated *in vivo* to have a precision of 0.19 mm or better for intervertebral translations and 1.1° or better for intervertebral rotations of the cervical spine.³ Motion data of C3 through C7 were included in the present analysis. A low-pass, 4th-order Butterworth filter was used to smooth the 6-DOF motion path of each bone (3 translations and 3 rotations), with the optimal filter frequency determined using residual analysis³⁸ (1.7 Hz for all flexion/extension trials and 1.5 Hz for all bend and rotation trials).

Disc Model

Markers were manually placed on the vertebral endplates of each 3D bone model to define the outer boundary of each intervertebral disc. Ten concentric rings consisting of between 100 (outer ring) and 11 (inner ring) nodes were automatically generated from

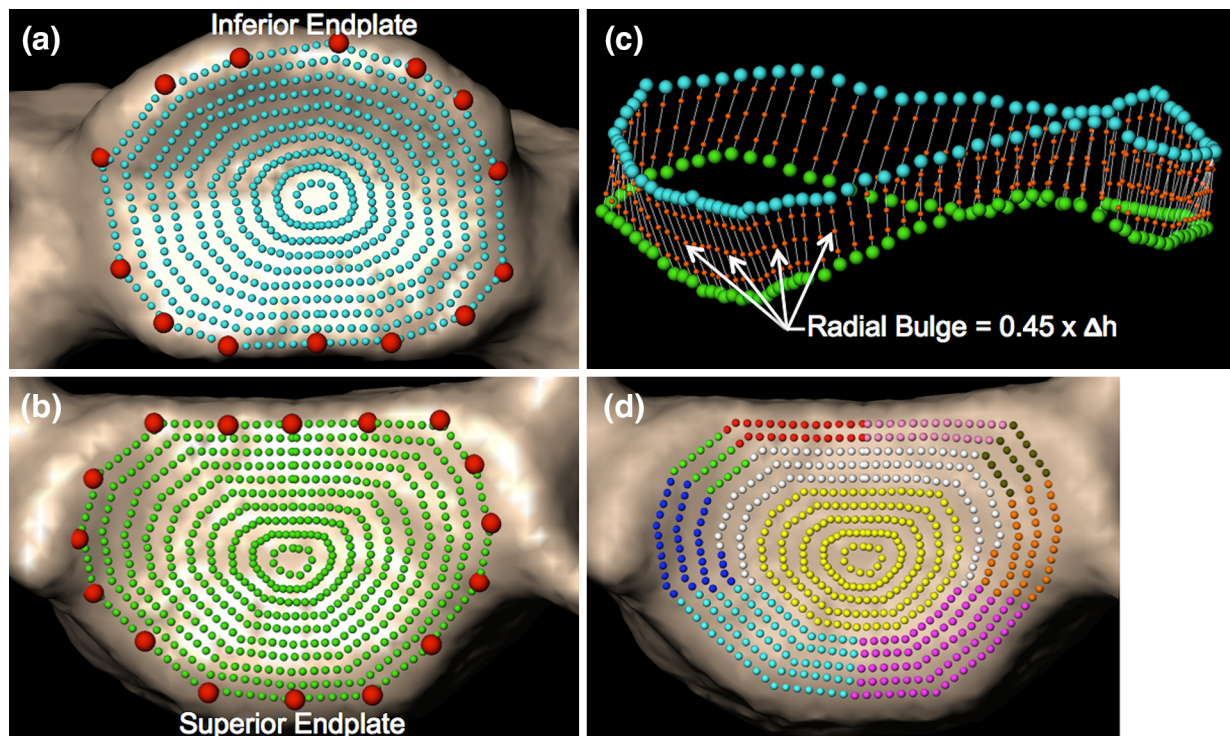


FIGURE 1. Creating the disc model. Markers were manually placed on the inferior (a) and superior (b) endplates of each bone (large red markers in a and b). An automated algorithm used these markers to create 10 concentric rings of nodes on each endplate (teal and green spheres). (c) Corresponding nodes on adjacent endplates were connected with line segments, and 3 intermediate nodes were created within each line segment (orange spheres in c). These intermediate nodes allowed for radial expansion and contraction of the disc during compression and distraction, respectively. Only the outermost ring of nodes is shown in c for clarity. (d) Each endplate node was assigned to an anatomic region according to its location: posterior annulus (red and pink), posterior-lateral annulus (green and brown), lateral annulus (blue and orange), anterior annulus (teal and maroon), and central nucleus (yellow).

these manually placed markers (Figs. 1a and 1b). Line segments connected corresponding nodes on adjacent endplates to model the intervertebral disc. Three additional nodes were created along each line segment, at 20, 50, and 80% of the distance between endpoints, in order to allow the line segments to deform in the radial direction during compression and distraction (Fig. 1c). Movement of the vertebrae (and the endpoint nodes rigidly attached to the endplates) was determined from the model-based tracking of each bone (described above). As the adjacent vertebral endplates moved closer together (and farther apart), the radial disc expansion and contraction was modeled according to the Poisson's ratio (ν) values for the annulus (0.45) and nucleus (0.499) that are commonly applied in cervical spine computational models^{20,24,39} (Fig. 1c).

Three components of disc strain (compression/distraction, radial, and shear) were calculated for each line segment used to model the disc (Fig. 2). Using the endplates of each bone in the static neutral position, an "average plane" was calculated between each pair of adjacent vertebrae (the "average plane" was deemed more appropriate than fitting a plane to either endplate

due to the trapezoidal shape of cervical vertebrae and the natural lordosis of the cervical spine). The orientation of this "average plane" was determined with respect to the inferior vertebra of each motion segment during the static neutral trial. During the dynamic movement trials, the orientation of the "average plane" remained fixed relative to the inferior vertebra. The compressive/distraction strain of each line segment comprising the disc was calculated for each frame of the dynamic movement using the equation: $\epsilon_{cd} = \frac{l_{d(perp)} - l_{s(perp)}}{l_{s(perp)}}$, where $l_{d(perp)}$ and $l_{s(perp)}$, were the dynamic and static length of the line segment perpendicular to the "average plane," respectively. The shear strain of each line segment comprising the disc was calculated similarly, using the equation: $\epsilon_{shear} = \frac{l_{d(par)} - l_{s(par)}}{l_{s(par)}}$, where $l_{d(par)}$ and $l_{s(par)}$, were the dynamic and static length of the line segment parallel to the "average plane," respectively. Finally, the radial strain in each line segment was calculated for each frame of the dynamic movement trial: $\epsilon_{radial} = \frac{disc_bulge}{l_{s(perp)}}$, where the disc bulge was equal to the Poisson's ratio times the change in perpendicular length of the line segment: $disc_bulge = \nu \times (l_{d(perp)} - l_{s(perp)})$.

Each line segment used to model the disc was assigned to one of 10 anatomic regions in order to create a crescent-shaped annulus²⁸ (Fig. 1d). For every frame of each dynamic movement trial, the average strain of all segments within each anatomic region was calculated. Then, the maximum of these average strains over the entire dynamic movement trial for each disc region was calculated. These peak strains were averaged across the two trials of each movement in order to determine the average peak strain within each region of each disc for every participant.

Statistical Analysis

A 3 × 4 × 5 repeated measures analysis of variance (ANOVA) was used to identify differences in average peak disc strain (compression/distraction, shear, and

radial strain, as defined above) according to head movement (lateral bending, flexion/extension, axial rotation), disc (C3–4, C4–5, C5–6, C6–7), and anatomic region within each disc (posterior, posterior–lateral, lateral, anterior, central nucleus). When the ANOVA test indicated that significant differences existed among levels of the main effects, significant differences were identified after applying the Bonferroni correction for multiple comparisons. Statistical analysis of the interaction between main effects (movement by disc, movement by region) is described in the appendix. Significance was set at $p < 0.05$ for all tests (IBM SPSS Statistics, Version 22.0).

Verification and Sensitivity Analysis

The computational model was verified to ensure that the underlying algorithms were implemented correctly. This was accomplished by a simulation experiment consisting of a simulated motion segment (bone + disc + bone) that was assigned a known kinematic movement pattern (± 1 , ± 2 , and ± 3 mm in compression/distraction and ± 1 , ± 2 , and ± 3 mm in anterior–posterior and left–right shear) in order to create known compression/distraction and shear deformation to the disc. The computational model was verified by calculating the absolute difference between the known strain due to the displacements and the calculated strain within each disc region.

The robustness of the model was evaluated by an intra- and inter-operator sensitivity analysis. For this analysis, on two separate occasions (at least 1 day apart), three operators manually placed markers on the vertebral endplates to define the disc boundaries for a motion segment in one participant. Motion segment kinematics from *in vivo* flexion/extension, rotation and lateral bend trials were used to deform each of the six

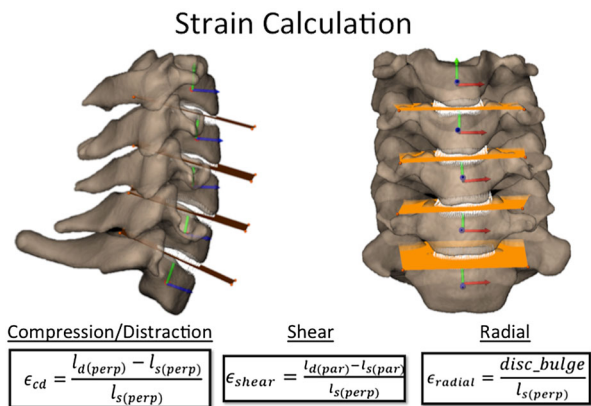


FIGURE 2. Sagittal (left) and anterior (right) views of the “average plane” for each motion segment in the static neutral position for one representative subject. Deformation perpendicular to the average plane created compression/distraction strain, deformation parallel to the average plane created shear strain, and deformation away from and toward the center of the disc created radial strain.

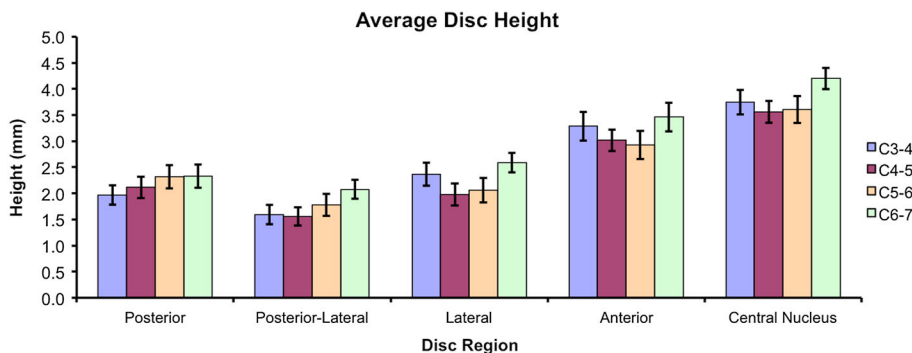


FIGURE 3. Average disc height in the static neutral position for 29 young healthy adults (mean ± 95% confidence interval). Disc height at the C3–4 (2.6 mm), C4–5 (2.4 mm) and C5–6 (2.5 mm) discs was significantly less than at the C6–7 disc (2.9 mm) (all $p \leq 0.001$). Significant differences were identified among disc regions (all $p < 0.001$ among all regions except posterior vs. lateral) (posterior: 2.2 mm, posterior–lateral: 1.8 mm, lateral: 2.2 mm, anterior: 3.2 mm, central nucleus: 3.8 mm).

disc models. Intra- and inter-operator sensitivity to manual marker placement was assessed by the differences in peak strain among disc models.

RESULTS

Model Verification and Sensitivity

For the simulated motion segment kinematics, the average absolute difference between the known and calculated disc strain over all disc regions and all simulated movements was less than 0.0005% for the compression, distraction and shear strains.

The average intra-operator absolute difference in peak compression, distraction and shear strain was 2.3, 3.2, and 3.7%, respectively, over all movements and all disc regions. The average inter-operator absolute difference in peak compression, distraction and shear strain was 4.2, 4.7, and 6.3%, respectively, over all movements and all disc regions.

All of the following quantitative results in the text and figures are expressed as mean \pm 95% confidence interval.

Static Disc Height

Overall average static disc height (i.e., $l_{s(\text{perp})}$, as described earlier) was significantly greater in the C6–7 disc (2.9 ± 0.2 mm), than in the C3–4 (2.6 ± 0.2 mm), C4–5 (2.4 ± 0.2 mm) and C5–6 discs (2.5 ± 0.2 mm) (all $p \leq 0.001$). Disc height ranged from 1.8 ± 0.1 mm in the posterior–lateral region to 3.8 ± 0.2 mm in the central nucleus, with significant differences identified among all regions (all $p < 0.001$) except for the posterior and lateral regions (Fig. 3).

Head and Intervertebral Range of Motion

Global head flexion/extension ROM was $119.0^\circ \pm 13.8^\circ$ during the flexion/extension movement (comprised of $56.5^\circ \pm 7.9^\circ$ in flexion and $63.6^\circ \pm 12.5^\circ$ in extension). Global head axial rotation ROM was

$142.8^\circ \pm 10.0^\circ$ during the axial rotation movement, and global head lateral bending ROM was $83.9^\circ \pm 11.0^\circ$ during the lateral bending movement. As expected, during flexion/extension, intervertebral movement occurred almost exclusively about the sagittal plane, while lateral bending and axial rotation induced coupled intervertebral motion (Table 1).

Peak Compression/Distracton Strain

Head Movement Differences

Maximum disc compression strain was significantly greater during the flexion/extension movement ($31.5 \pm 2.5\%$) than during the lateral bend movement ($27.3 \pm 2.4\%$; $p = 0.021$), while compression during axial rotation ($28.4 \pm 2.6\%$) was not significantly different from either flexion/extension or bending. Peak disc distraction strain was greater during the lateral bend movement ($56.9 \pm 4.9\%$) than during the rotation ($45.6 \pm 3.8\%$; $p < 0.001$) and flexion/extension movement ($35.7 \pm 3.9\%$; $p < 0.001$ vs. rotation and vs. flexion/extension) (Fig. 4a).

Disc Level Differences

Peak compression strain was greatest in the C4–5 disc ($33.0 \pm 4.0\%$) and smallest in the C6–7 disc ($26.2 \pm 3.1\%$; $p = 0.014$), with no significant differences between these discs and the C3–4 ($29.6 \pm 3.0\%$) and C5–6 ($27.6 \pm 3.2\%$) discs. Peak distraction strain progressively decreased from superior to inferior discs (C3–4: $54.1 \pm 7.7\%$, C4–5: $48.9 \pm 7.5\%$, C5–6: $43.7 \pm 7.7\%$, and C6–7: $37.5 \pm 5.4\%$), with the C3–4 and C4–5 significantly greater than C6–7 ($p = 0.002$ and $p = 0.049$, respectively) (Fig. 4b).

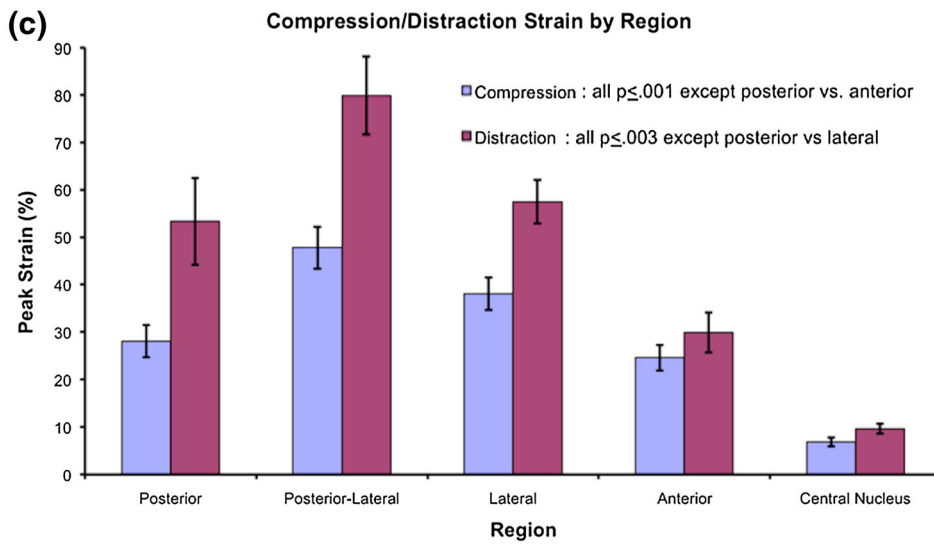
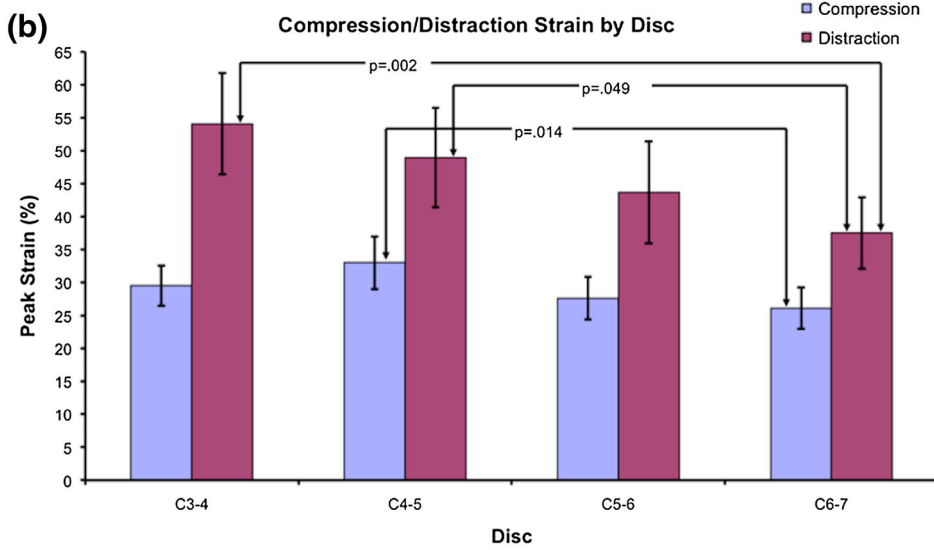
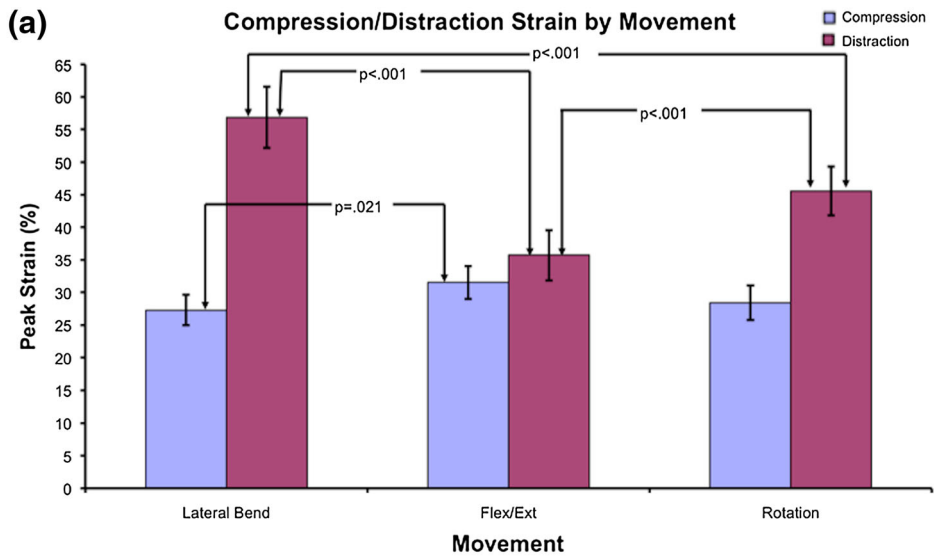
Disc Region Differences

Significant differences in peak compression strain were identified among disc regions, with the greatest compressive strain occurring in the posterior–lateral region ($47.8 \pm 4.4\%$; all $p \leq 0.001$), followed by the

TABLE 1. Rotation range of motion components during dynamic flexion/extension, axial rotation, and lateral bending movements in 29 healthy young adults.

Motion segment	Flexion/extension			Axial rotation			Lateral bending		
	Flex/ext	Rotation	Bend	Flex/ext	Rotation	Bend	Flex/ext	Rotation	Bend
C3–C4	17.1 ± 2.5	1.9 ± 0.5	2.3 ± 0.5	5.1 ± 1.2	11.8 ± 1.6	13.4 ± 1.6	6.9 ± 2.4	11.6 ± 1.6	14.3 ± 2.1
C4–C5	19.5 ± 2.6	1.8 ± 0.5	2.0 ± 0.5	4.7 ± 1.5	11.3 ± 1.3	12.8 ± 2.1	5.1 ± 1.7	9.4 ± 1.9	13.1 ± 2.4
C5–C6	19.7 ± 2.8	1.7 ± 0.5	2.1 ± 0.5	4.5 ± 1.5	9.3 ± 1.4	11.7 ± 2.3	4.6 ± 1.4	6.7 ± 1.6	12.3 ± 2.4
C6–C7	15.8 ± 3.7	1.6 ± 0.5	2.4 ± 0.8	3.4 ± 0.9	6.5 ± 1.3	12.6 ± 2.4	3.9 ± 1.2	5.5 ± 1.7	14.5 ± 3.0
Head–torso	119.0 ± 10.5	8.5 ± 2.5	9.3 ± 3.3	10.5 ± 2.5	142.8 ± 10.0	51.4 ± 25.6	12.9 ± 4.3	29.7 ± 10.9	83.9 ± 11.0

Mean (\pm 95% CI) values are in degrees. This data originally appeared in Anderst *et al.* 2015.



◀ **FIGURE 4. Peak compression/distraction strain. (a) By movement, (b) by disc level, and (c) by disc region. Error bars indicate upper and lower 95% confidence intervals for the mean.**

lateral region ($38.0 \pm 3.4\%$; all $p \leq 0.001$), the posterior and anterior regions (28.1 ± 3.4 and $24.6 \pm 2.7\%$, respectively), and the central nucleus ($6.9 \pm 0.9\%$; all $p < 0.001$). Significant differences in maximum distraction strain were identified among disc regions, with the greatest distraction strain occurring in the posterior–lateral region ($79.9 \pm 8.3\%$; all $p < 0.001$), followed by the lateral and posterior regions (57.5 ± 4.6 and $53.3 \pm 9.1\%$, respectively), the anterior region ($29.9 \pm 4.2\%$; all $p \leq 0.003$), and the central nucleus ($9.7 \pm 1.1\%$; all $p < 0.001$) (Fig. 4c).

A movie demonstrating disc compression/distraction strain during lateral bending, flexion/extension and axial rotation is included in the supplemental materials. Results related to interactions among main effects for peak compression and distraction strains (head movement by disc level and head movement by disc region) appear in the Appendix.

Peak Shear Strain

Head Movement Differences

Peak shear strain was significantly greater during the flexion/extension movement ($86.2 \pm 8.4\%$) than during the lateral bend ($65.7 \pm 7.5\%$; $p < 0.001$) and axial rotation ($63.9 \pm 6.1\%$; $p < 0.001$) movements (Fig. 5a).

Disc Level Differences

Peak shear strain was significantly greater in the C3–4 ($82.7 \pm 10.9\%$), C4–5 ($81.8 \pm 9.2\%$), and C5–6 ($69.3 \pm 9.5\%$) discs than in the C6–7 disc ($54.0 \pm 5.7\%$; all $p \leq 0.004$) (Fig. 5b).

Disc Region Differences

Maximum shear strain varied significantly among disc regions, with the largest shear strain in the posterior–lateral region ($109.2 \pm 12.3\%$; all $p \leq 0.001$), followed by the lateral and posterior regions (89.4 ± 9.0 and $78.5 \pm 11.9\%$, respectively; all $p \leq 0.001$ vs. other regions), then the anterior region ($46.7 \pm 4.3\%$; $p \leq 0.001$ vs. all other regions), and finally the central nucleus ($35.9 \pm 2.6\%$; $p < 0.001$ vs. all other regions) (Fig. 5c).

A movie demonstrating disc shear strain during lateral bending, flexion/extension and axial rotation is included in the supplemental materials. Results related to interactions among main effects for peak shear

strains (head movement by disc level and head movement by disc region) appear in the Appendix.

Peak Radial Strain

In the computational model, radial expansion and contraction strain were directly related to disc compression/distraction strain ($\epsilon_{\text{radial}} = \nu \times \epsilon_{\text{cd}}$). Therefore, each statistically significant difference in peak disc compression and distraction strain had a corresponding statistically significant result for peak radial expansion and contraction strain. A movie demonstrating radial disc strain during flexion/extension is included in the supplemental materials, and peak radial strain results appear in the Appendix.

DISCUSSION

The aim of this study was to assess the effects of head movement (flexion/extension, lateral bending, and axial rotation), disc level (C3–4 to C6–7), and disc region (posterior, posterior–lateral, lateral, and anterior annulus, and central nucleus) on peak cervical disc strain. This was accomplished by developing a subject-specific computational model of each cervical disc. The computational models were driven by *in vivo*, dynamic kinematics recorded using a biplane radiography system and model-based tracking algorithm. The computational modeling software was verified by a simulation experiment, and the robustness of the model was assessed by a sensitivity analysis.

In order to provide perspective on the accuracy and robustness of the conclusions drawn from a computational model, it is important to verify, validate and assess the sensitivity of the model.^{2,17} The simulation experiment served to verify that the computational algorithms to calculate disc strain were, in fact, implemented correctly. Due to technical challenges and ethical concerns, it is currently impractical to directly measure cervical disc tissue strains during *in vivo* functional loading in humans in order to create a “gold standard” for validating the model. Therefore, the validation of the current computational model was limited to the input kinematics used to drive the model, which have been previously validated *in vivo* to be 0.19 mm or better.³ Given this kinematic accuracy and the average disc height (2.63 mm), the precision in estimating strain was, on average, 7% or better. Finally, the sensitivity analysis demonstrated that the variation in peak strain due to different operators manually placing disc boundary markers (6.3% or less) was relatively small in comparison to the calculated peak disc strains. In practice, all disc boundary markers were placed by the same operator (WA). The

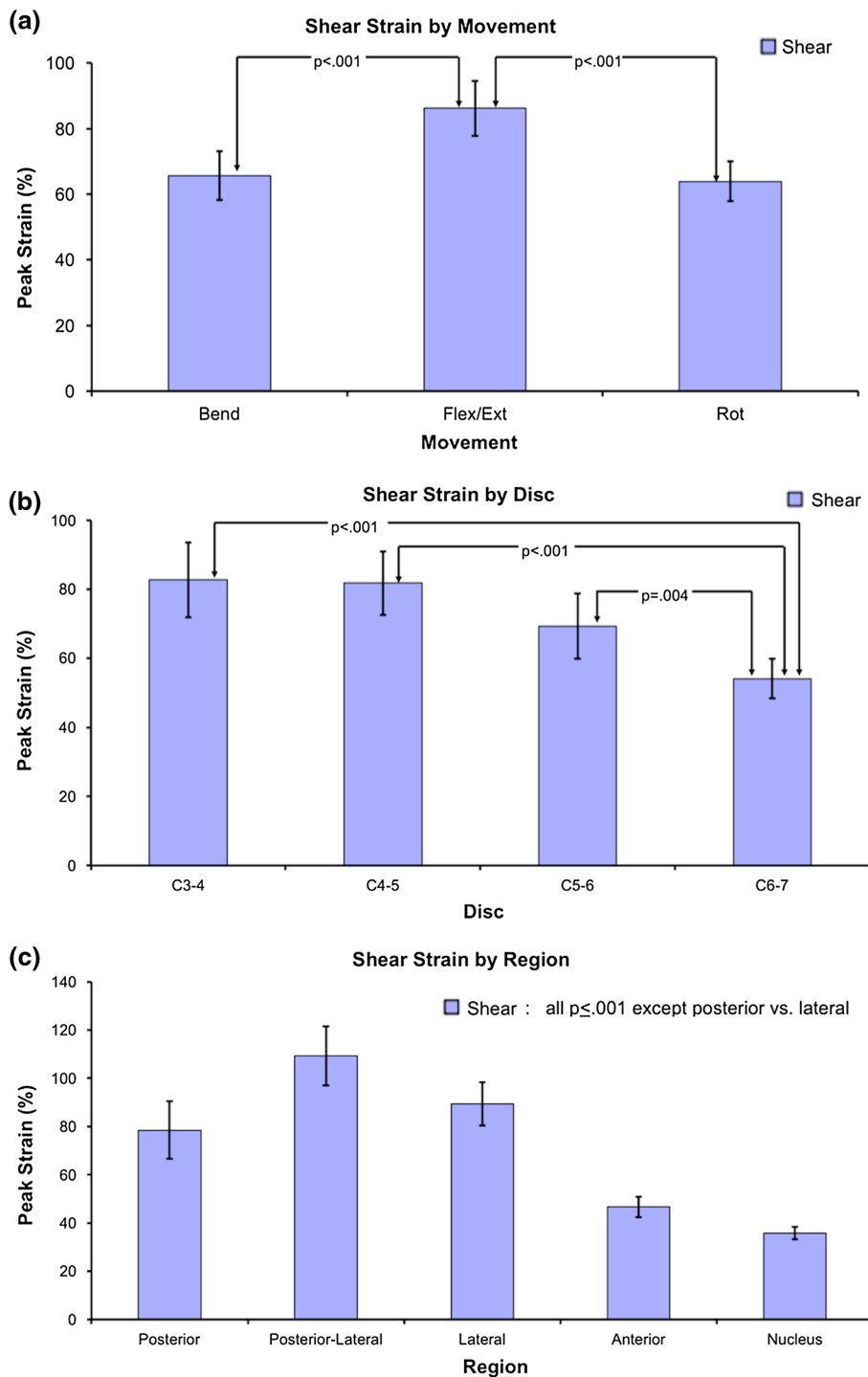


FIGURE 5. Peak shear strain. (a) By movement, (b) by disc level, and (c) by disc region. Error bars indicate upper and lower 95% confidence intervals for the mean.

average variation in peak strain due to manually placing disc boundary markers by this operator was 2.3%.

A key parameter for estimating disc strain is the disc height in the static neutral position. In the present

study, average disc height ranged from 1.8 mm in the posterior-lateral annulus to 3.8 mm in the central nucleus. These values fall within the previously reported range of average values for cervical disc height. Measurements from sagittal plane radiographs

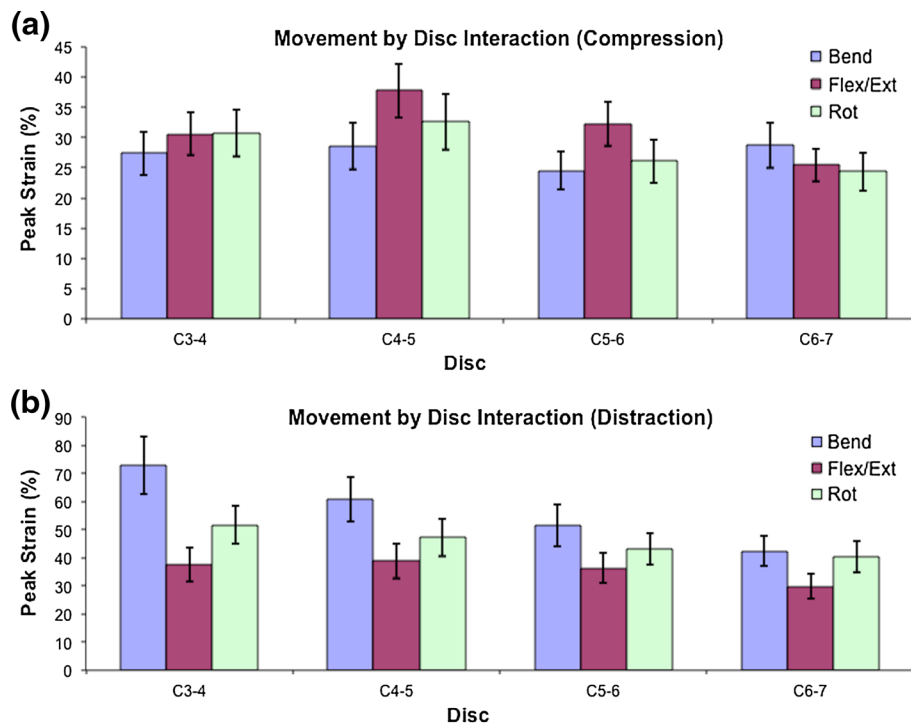


FIGURE 6. Peak compression strain (a) and peak distraction strain (b) for each head movement and disc level. Note that the vertical scales are different in (a) and (b). Significant differences among disc levels within each head movement are identified in the appendix text. Error bars indicate upper and lower 95% confidence intervals for the mean.

(that may not have accounted for magnification) indicated anterior disc height in the cervical spine ranged between 4.7 and 5.5 mm, while posterior disc height ranged from 3.0 to 3.5 mm in 141 young adult males.¹⁴ On the other end of the spectrum, using MRI, average C4–5 to C6–7 disc height ranged between 2.1 and 2.6 mm in the anterior disc, between 2.6 and 2.9 in the middle disc, and between 1.5 and 1.9 in the posterior disc in 43 subjects between 20 and 60 years of age.¹⁸ A study that used sagittal reconstructions from CT scans reported disc heights between these two extremes, with disc height in the nucleus region averaging between 2.6 and 3.7 mm in 100 middle-aged adults (average age 47 years).²⁵ Differences in reported disc height may be due to a number of factors, including subject age, subject position during imaging (prone for CT or MRI vs. upright during a radiograph), and measurement technique (manual identification of 4–5 bone landmarks on the 2D medical image vs. automated measurements over the entire 3D surface of each endplate).

The Effect of Head Movement

It was hypothesized that cervical disc strains are higher during flexion/extension than during the combined motion that occurs during bending and rotation.

The results indicated little variation in peak disc compression strain among head movements (range 27–31%). In comparison, peak disc distraction strain was larger and more variable across head movements (range 36–57%). The substantially larger peak distraction strains during lateral bending and rotation (in comparison to peak compression strains during all movements and peak distraction strain in flexion/extension) demonstrate that in order to assess disc response to the full range of compression and distraction strain experienced *in vivo*, in addition to flexion/extension, multi-planar movements of bending and rotation must be included in the testing protocol. Peak shear strain was larger than peak compression and peak distraction strain during all head movements (range 64–86%), and was greatest during the flexion/extension movement. Therefore, the hypothesis that peak disc strains are highest during flexion/extension was supported when considering shear and compression strains, however, peak distraction strains were highest during lateral bending.

The Effect of Disc Level

It was hypothesized that disc strains are greatest at the C5–6 and C6–7 discs (since degenerative changes occur most frequently at these levels¹³) and smallest at

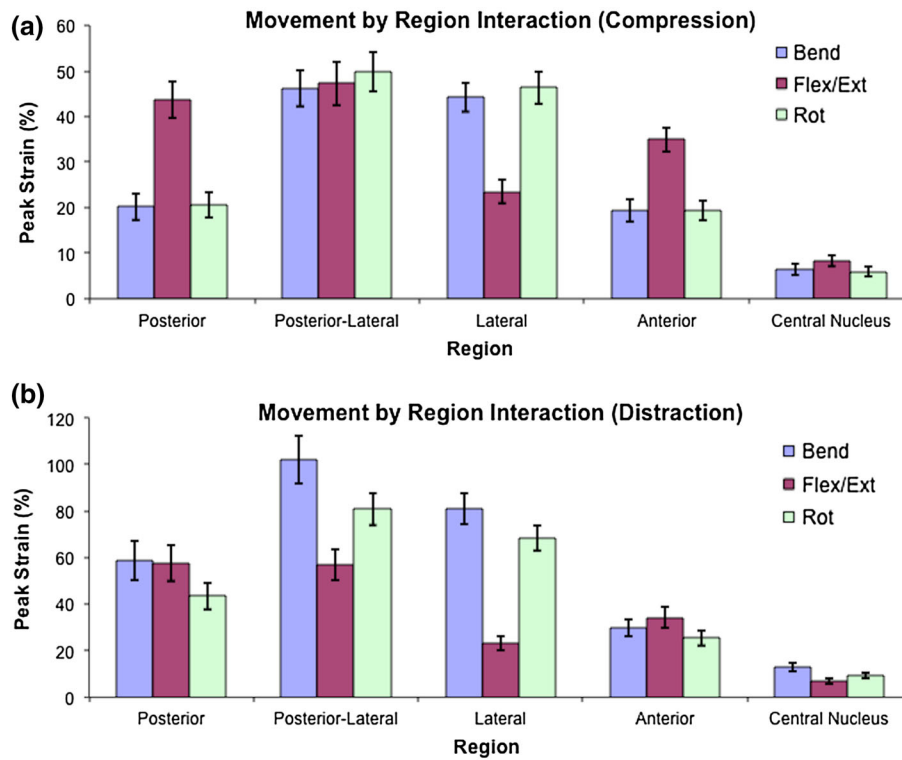


FIGURE 7. Peak compression strain (a) and peak distraction strain (b) for each head movement and disc region. Note that the vertical scales are different in (a) and (b). Significant differences among disc regions within each head movement are identified in the text. Error bars indicate upper and lower 95% confidence intervals for the mean.

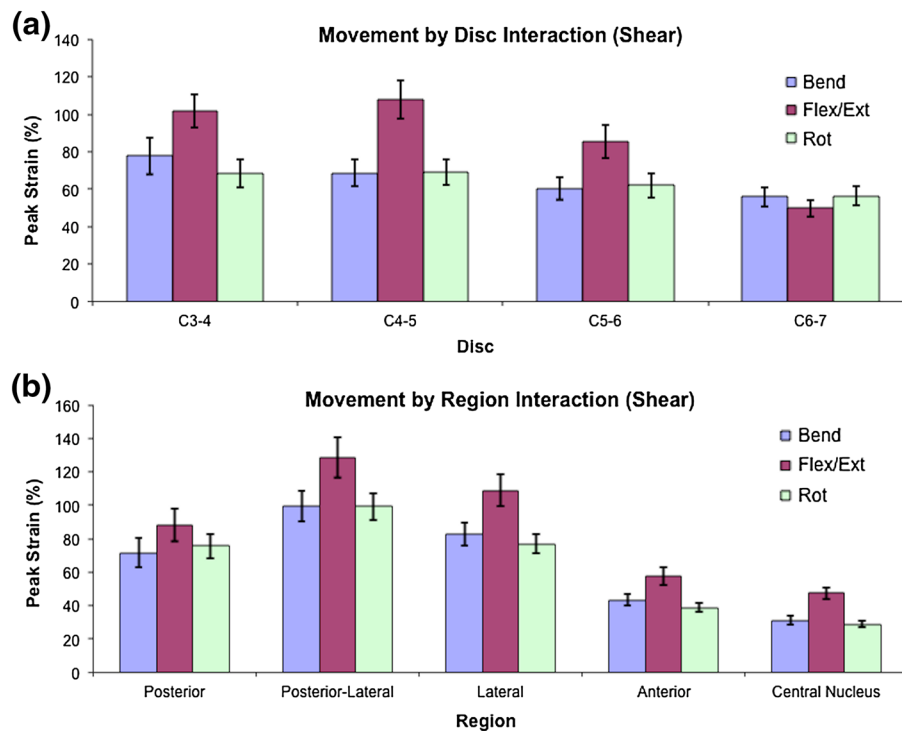


FIGURE 8. Movement by disc interaction for peak shear strain (a) and movement by disc region interaction for peak shear strain (b). Significant differences among discs and among disc regions within each head movement are identified in the text. Error bars indicate upper and lower 95% confidence intervals for the mean.

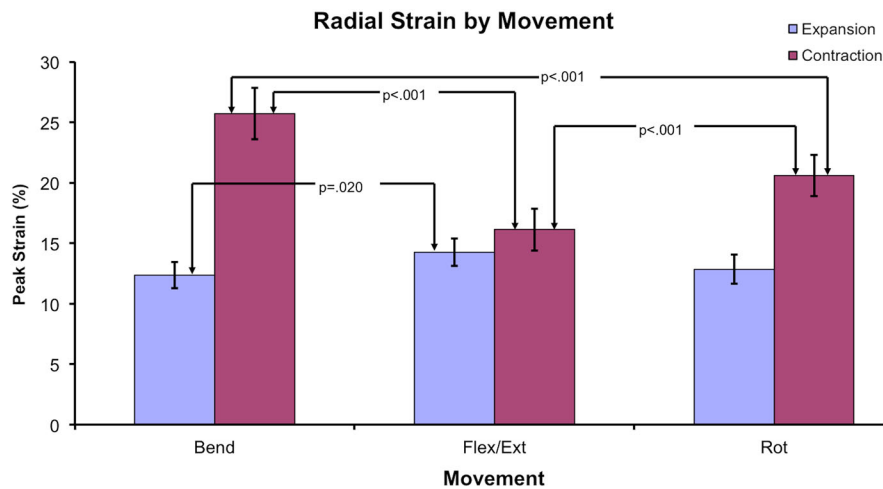


FIGURE 9. Peak expansion and contraction radial strains by movement. Error bars indicate upper and lower 95% confidence intervals for the mean. Note the correspondence to Fig. 4a.

the C3–4 and C4–5 discs. Peak compression strain was greatest in the C4–5 disc, however, little variation was observed among discs (range 26–33%). In comparison, peak distraction strain was larger than peak compression strain in each disc, and peak distraction strain was largest at C3–4 and decreased sequentially to C6–7 (range 38–54%). Peak shear strain was larger than peak compression and distraction strain in all discs (range 64–86%), and was greatest in the C3–4 and C4–5 discs. Therefore, the hypothesis that peak disc strain occurs in C5–6 and C6–7 discs was not supported when considering compression, distraction, and shear strains. In fact, peak compression, distraction, and shear strains were all significantly less in the C6–7 disc than in the C4–5 disc. Thus, there does not appear to be a relationship between peak tissue strain and clinically observed disc-level differences in the incidence of symptomatic degeneration. A potential alternative explanation for level-dependent differences in disc degeneration is that the disc stress may be greater at the C5–6 and C6–7 discs due to the natural lordotic curvature of the cervical spine, which peaks at the level of C5–6.

The Effect of Disc Region

It was hypothesized that disc strains are higher in the posterior–lateral annulus than in the posterior, lateral and anterior annulus, and in the nucleus. This study demonstrated that peak compression strain varied considerably among disc regions (range 7–48%) and was greatest in the posterior–lateral annulus. Peak disc distraction strain was also largest in the posterior–lateral annulus, and in comparison to peak compression strain, peak distraction strain was larger and encompassed a greater range of values across disc regions (range 10–

80%). Peak shear strain was also greatest in the posterior–lateral region, and peak shear strain was larger than peak compression and distraction strain in all disc regions (range 36–109%). Therefore, the hypothesis that peak disc strains are highest in the posterior–lateral annulus was supported for compression, distraction and shear strains. This result corresponds to the clinical observation of increased incidence of symptomatic pathology in the posterior–lateral region of the cervical discs.²³

Comparison to Previous Research

The literature on *in vivo* disc strain is sparse. Average compression, distraction, and shear strains have been calculated over the central 1/3rd of the disc during the flexion/extension motion, with maximum compression and distraction strains in the anterior and posterior annulus reaching 20%, and maximum shear deformation up to 33%.⁴ While this previous study reported mean strain values at specific intervertebral orientations, the current study reported peak strain values over the entire movement. Differences between the results of the studies may also be due to the decreased range of motion in older participants (average age 46 ± 9 years in the previous study). Another previous study using pre-operative flexion/extension radiographs of cervical fusion patients determined that pre-operative shear strain averaged 5–7% in segments adjacent to the surgical site.²⁷ However, the magnitude of the pre-surgical adjacent segment range of motion was not provided, making it difficult to interpret this finding. Finally, one study used cineradiography to estimate maximum lumbar disc compressive and shear strains of 35 and 60%, respectively, at full flexion.²¹

Study Strengths and Limitations

The strengths of this study include highly precise kinematic data from a relatively large sample of individuals who performed multiple trials of *in vivo*, dynamic, three-dimensional head flexion/extension, lateral bending, and axial rotation movements. The significance of these individual study characteristics cannot be understated. The sub-millimeter accuracy of the kinematics used to drive the computational model was critical for accurately estimating tissue strain. Also, the unique motion characteristics of each individual as they performed multi-planar head motions, and the muscular and inertial loads applied during these motions, cannot be replicated using cadaver specimens and mechanical loading devices. Another strength of the study was that the analysis ventured beyond the conventional assessment of spine mechanics, which traditionally focus on bone kinematics such as the quantity of motion (i.e., range of motion) and quality of motion (i.e., center of rotation) at each motion segment.^{5,26} These common kinematic parameters are useful for assessing changes in bone movement related to age, therapeutic interventions, and surgical procedures. However, due to the simultaneous six degree-of-freedom movements that occur at each motion segment during dynamic loading, it is impractical to infer disc mechanics based solely on these common bone kinematic measurements. The advantage of including a computational model of each disc is that disc deformation can be easily characterized, interpreted and visualized during the complex, multi-planar movements at each motion segment. Additionally, it was important that the model was computationally efficient, considering that 6 movement trials were analyzed for each of the 29 subjects. Calculating disc deformation over an entire dynamic movement trial required less than 1 min using a laptop computer, whereas a finite element model containing 5 bones and 4 intervertebral discs would require several hours or more to process just one dynamic movement trial.

A limitation of the study is that the true strain in the tissues in the static neutral position was not known. Therefore, the strain values reported are *relative* strain values, and are estimates of the change in tissue strain with respect to the static neutral position. Further, this study estimated strain in the disc tissue, and the results may not necessarily be reflective of the micromechanical stimuli experienced at the cellular level.⁹ However, the peak strains reported here still serve as a valuable reference for assessing disc mechanobiology using entire motion segments.¹⁵ The computational model employed is limited to estimating tissue strain, and cannot assess disc stress. Disc stress could be estimated using a combination of precise bone kinematics and an alternative computational analysis technique, such as a finite ele-

ment analysis or discrete element analysis. An additional limitation is that this study focused on peak strain values (rather than average strains, or strains in the mid-range of motion, for example). Peak strains were assessed in order to establish boundaries for maximal *in vivo* physiologic strain values that are achieved during pain-free, full range of motion movements. Finally, due to the changes in cervical spine kinematics that occur with age,^{34,40} the results of this study are applicable only to the young healthy adult cervical spine.

Implications for In Vitro Disc Mechanobiology Studies

Biological responses to mechanical stimuli may be identified through *in vitro* mechanobiology studies. *In vitro* loading paradigms that aim to replicate *in vivo* “physiologic” and “overload” compression, distraction, and shear tissue strain during multi-dimensional loading on cervical disc tissues can use the boundary conditions provided by the present study to appropriately design loading regimens to assess biologic response to physiologic disc deformations. Additionally, the biofidelity of tissue explant loading paradigms can be improved by applying the disc region-specific strains reported here.

ELECTRONIC SUPPLEMENTARY MATERIAL

The online version of this article (doi:[10.1007/s10439-015-1424-2](https://doi.org/10.1007/s10439-015-1424-2)) contains supplementary material, which is available to authorized users.

APPENDIX

The body of the manuscript tests hypotheses and presents results related to the main effect variables (head movement, disc level, and disc region). The interactions between head movement and disc level and between head movement and disc region are presented here in the appendix to provide the curious reader a more detailed presentation of the study results. In addition, the appendix includes an example of the radial disc deformations estimated by the computational model.

METHODS

Statistical Analysis for Interactions Among Main Effects

When the repeated-measures ANOVA test indicated that significant interactions existed between main effects (movement by disc, movement by region), the Tukey HSD *post hoc* test was used to test for differ-

ences. Significance was set at $p < 0.05$ for all tests (IBM SPSS Statistics, Version 22.0).

RESULTS

Peak Compression/Distracton Strain

Head Movement by Disc Level Interactions

The head movement by disc level interactions were significant for peak compression strain ($p = 0.002$) and peak distraction strain ($p < 0.001$), indicating that the pattern of peak strain changed across discs according to head movement. During flexion/extension, peak compression strain in the C4–5 disc ($37.8 \pm 4.5\%$) was significantly greater than in the C3–4 ($30.6 \pm 3.5\%$; $p = 0.031$) and C6–7 ($25.4 \pm 2.7\%$; $p < 0.001$) discs, while peak compression strain in the C5–6 disc ($32.3 \pm 3.7\%$) was significantly greater than the C6–7 disc ($p = 0.044$). In contrast, no significant differences in maximum compression strain were observed among discs during lateral bending (all $p \geq 0.380$). During axial rotation, only peak compression strain in the C4–5 disc ($32.6 \pm 4.6\%$) was significantly greater than in the C6–7 disc ($24.4 \pm 3.2\%$; $p = 0.15$) (Fig. 6a in Appendix).

Peak distraction strain was not significantly different among discs during the flexion/extension movement (range $38.9 \pm 6.2\%$ at C4–5 to $29.8 \pm 4.4\%$ at C6–7; all $p \geq 0.103$) or during rotation (range: $51.7 \pm 6.9\%$ at C3–4 to $40.4 \pm 5.5\%$ at C6–7; all $p \geq 0.052$). In contrast, during lateral bending, peak distraction strain decreased linearly ($p \leq 0.001$) from C3–4 ($72.8 \pm 10.1\%$) to C6–7 ($42.5 \pm 5.5\%$), with peak distraction at C3–4 and C4–5 ($60.8 \pm 8.0\%$) significantly greater than at C6–7 ($p < 0.001$ and $p = 0.007$, respectively), and peak distraction at C3–4 significantly greater than at C5–6 ($51.5 \pm 7.5\%$; $p = 0.001$) (Fig. 6b in Appendix).

Head Movement by Disc Region Interactions

The movement by region interactions were significant for peak compression ($p < 0.001$) and distraction ($p < 0.001$) strains, indicating that the pattern of peak compression/distracton strain changed across disc regions according to head movement. Peak compressive strains during the lateral bending and axial rotation motions were nearly identical across all disc regions, with the maximum strains in the posterior–lateral and lateral disc regions significantly greater than in all other regions (all $p < 0.001$). During flexion/extension, on the other hand, peak compression strain was significantly greater in the posterior–lateral and posterior regions than in all other regions (all

$p < 0.001$), with the anterior region greater than the lateral and central nucleus regions (all $p < 0.001$) (Fig. 7a in Appendix).

Peak distraction strains during the lateral bending and axial rotation motions followed similar patterns across disc regions, with the maximum strains significantly different among all regions (all $p \leq 0.005$). During the flexion/extension movement peak distraction strain was significantly greater in the posterior–lateral and posterior regions than in all other regions (all $p \leq 0.005$) (Fig. 7b in Appendix).

Peak Shear Strain

Head Movement by Disc Level Interactions

The head movement by disc level interactions were significant for peak shear strain ($p < 0.001$) indicating that the pattern of peak strain changed across discs during different head movements. Peak shear strain decreased linearly from the C3–4 to C6–7 disc for each movement (bend: $p = 0.004$, flexion/extension: $p < 0.001$, rotation $p = 0.006$). However, the range of shear strains across discs was much larger during flexion/extension (range 107.8 ± 10.2 to $49.8 \pm 4.5\%$) than during lateral bending (range 77.8 ± 9.8 to $56.0 \pm 5.2\%$) or rotation (range 68.9 ± 6.8 to $56.3 \pm 5.1\%$) movements (Fig. 8a in Appendix).

Head Movement by Disc Region Interactions

The head movement by disc region interactions were significant for peak shear strain ($p < 0.001$). During the lateral bending and rotation movements, peak shear strain was significantly different among all disc regions (all $p < 0.001$) except for the posterior vs. lateral annulus regions (all $p \geq 0.164$) and the anterior annulus vs. central nucleus regions (all $p \geq 0.085$). During the flexion/extension movement, peak shear strain was significantly different among all disc regions (all $p \leq 0.012$) except for the anterior annulus vs. central nucleus region ($p = 0.446$) (Fig. 8b in Appendix).

Peak Radial Strain

In the computational model, radial expansion and contraction strain were directly related to disc compression/distracton strain ($\epsilon_{\text{radial}} = \nu \times \epsilon_{\text{cd}}$) and the radial strains were not influenced by shearing between endplates. Therefore, each statistically significant difference in peak disc compression and distraction strain had a corresponding statistically significant result for peak radial expansion and contraction strain. For example, peak radial expansion strain was significantly

greater during the flexion/extension movement ($14.3 \pm 1.1\%$) than during the lateral bend movement ($12.4 \pm 1.1\%$; $p = 0.020$), while peak expansion during axial rotation ($12.9 \pm 1.2\%$) was not significantly different from either flexion/extension or bending (Fig. 9 in Appendix). Similarly, the peak contraction results corresponded to the peak distraction results presented in Fig. 1a. As a point of reference, given the average disc height over all discs and regions (2.6 mm), a 10% radial strain corresponded to approximately 0.26 mm of disc expansion/contraction.

ACKNOWLEDGMENTS

This study was supported by Synthes Spine. The authors have no professional or financial affiliations that may be perceived to have biased the manuscript.

REFERENCES

- ¹Adams, M. A., P. Dolan, and D. S. McNally. The internal mechanical functioning of intervertebral discs and articular cartilage, and its relevance to matrix biology. *Matrix Biol.* 28(7):384–389, 2009.
- ²Anderson, A. E., B. J. Ellis, and J. A. Weiss. Verification, validation and sensitivity studies in computational biomechanics. *Comput. Methods Biomech. Biomed. Engin.* 10(3):171–184, 2007.
- ³Anderst, W. J., E. Baillargeon, W. F. Donaldson, 3rd, J. Y. Lee, et al. Validation of a noninvasive technique to precisely measure in vivo three-dimensional cervical spine movement. *Spine (Phila Pa 1976)* 36(6):E393–E400, 2011.
- ⁴Anderst, W., W. Donaldson, J. Lee, and J. Kang. Cervical disc deformation during flexion-extension in asymptomatic controls and single-level arthrodesis patients. *J. Orthop. Res.* 31(12):1881–1889, 2013.
- ⁵Anderst, W. J., W. F. Donaldson, 3rd, J. Y. Lee, and J. D. Kang. Three-dimensional intervertebral kinematics in the healthy young adult cervical spine during dynamic functional loading. *J. Biomech.* 48:1286–1293, 2015.
- ⁶Anderst, W., R. Zauel, J. Bishop, E. Demps, et al. Validation of three-dimensional model-based tibio-femoral tracking during running. *Med. Eng. Phys.* 31(1):10–16, 2009.
- ⁷Bey, M. J., R. Zauel, S. K. Brock, and S. Tashman. Validation of a new model-based tracking technique for measuring three-dimensional, in vivo glenohumeral joint kinematics. *J. Biomech. Eng.* 128(4):604–609, 2006.
- ⁸Biswas, D., J. E. Bible, M. Bohan, A. K. Simpson, et al. Radiation exposure from musculoskeletal computerized tomographic scans. *J. Bone Joint Surg. Am.* 91(8):1882–1889, 2009.
- ⁹Bruehlmann, S. B., P. A. Hulme, and N. A. Duncan. In situ intercellular mechanics of the bovine outer annulus fibrosus subjected to biaxial strains. *J. Biomech.* 37(2):223–231, 2004.
- ¹⁰Chan, S. C., S. J. Ferguson, and B. Gantenbein-Ritter. The effects of dynamic loading on the intervertebral disc. *Eur. Spine J.* 20(11):1796–1812, 2011.
- ¹¹Davis, M. A., T. Onega, W. B. Weeks, and J. D. Lurie. Where the United States spends its spine dollars: expenditures on different ambulatory services for the management of back and neck conditions. *Spine (Phila Pa 1976)* 37(19):1693–1701, 2012.
- ¹²Fazel, R., H. M. Krumholz, Y. Wang, J. S. Ross, et al. Exposure to low-dose ionizing radiation from medical imaging procedures. *N. Engl. J. Med.* 361(9):849–857, 2009.
- ¹³Friedenberg, Z. B., and W. T. Miller. Degenerative disc disease of the cervical spine. *J. Bone Joint Surg. Am.* 45:1171–1178, 1963.
- ¹⁴Gilad, I., and M. Nissan. A study of vertebra and disc geometric relations of the human cervical and lumbar spine. *Spine (Phila Pa 1976)* 11(2):154–157, 1986.
- ¹⁵Hartman, R. A., T. Yurube, K. Ngo, N. E. Merzlak, et al. Biological responses to flexion/extension in spinal segments ex vivo. *J. Orthop. Res.* 33:1255–1264, 2015.
- ¹⁶Hattori, S., H. Oda, and U. Kawai. Cervical intradiscal pressure in movements and traction of the cervical spine. *Z. Orthop.* 119:568–569, 1981.
- ¹⁷Hicks, J. L., T. K. Uchida, A. Seth, A. Rajagopal, et al. Is my model good enough? Best practices for verification and validation of musculoskeletal models and simulations of movement. *J. Biomech. Eng.* 137(2):020905, 2015.
- ¹⁸Humphreys, S. C., S. D. Hodges, A. Patwardhan, J. C. Eck, et al. The natural history of the cervical foramen in symptomatic and asymptomatic individuals aged 20–60 years as measured by magnetic resonance imaging. A descriptive approach. *Spine (Phila Pa 1976)* 23(20):2180–2184, 1998.
- ¹⁹Iatridis, J. C., J. J. MacLean, P. J. Roughley, and M. Alini. Effects of mechanical loading on intervertebral disc metabolism in vivo. *J. Bone Joint Surg. Am.* 88(Suppl 2):41–46, 2006.
- ²⁰Kallemeyn, N., A. Gandhi, S. Kode, K. Shivanna, et al. Validation of a C2–C7 cervical spine finite element model using specimen-specific flexibility data. *Med. Eng. Phys.* 32(5):482–489, 2010.
- ²¹Kanayama, M., S. Tadano, K. Kaneda, T. Ukai, et al. A cineradiographic study on the lumbar disc deformation during flexion and extension of the trunk. *Clin. Biomech. (Bristol, Avon)* 10(4):193–199, 1995.
- ²²Kirkaldy-Willis, W. H., J. H. Wedge, K. Yong-Hing, and J. Reilly. Pathology and pathogenesis of lumbar spondylosis and stenosis. *Spine (Phila Pa 1976)* 3(4):319–328, 1978.
- ²³Kokubun, S., and Y. Tanaka. Types of cervical disc herniation and relation to myelopathy and radiculopathy. *J. Back Musculoskelet. Rehabil.* 5(2):145–154, 1995.
- ²⁴Kumaresan, S., N. Yoganandan, F. A. Pintar, and D. J. Maiman. Finite element modeling of the cervical spine: role of intervertebral disc under axial and eccentric loads. *Med. Eng. Phys.* 21(10):689–700, 1999.
- ²⁵Kwon, B. K., F. Song, W. B. Morrison, J. N. Grauer, et al. Morphologic evaluation of cervical spine anatomy with computed tomography: anterior cervical plate fixation considerations. *J. Spinal Disord. Tech.* 17(2):102–107, 2004.
- ²⁶Lin, C. C., T. W. Lu, T. M. Wang, C. Y. Hsu, et al. In vivo three-dimensional intervertebral kinematics of the subaxial cervical spine during seated axial rotation and lateral bending via a fluoroscopy-to-CT registration approach. *J. Biomech.* 47(13):3310–3317, 2014.

- ²⁷Matsunaga, S., S. Kabayama, T. Yamamoto, K. Yone, *et al.* Strain on intervertebral discs after anterior cervical decompression and fusion. *Spine* 24(7):670–675, 1999.
- ²⁸Mercer, S., and N. Bogduk. The ligaments and annulus fibrosus of human adult cervical intervertebral discs. *Spine (Phila Pa 1976)* 24(7):619–626, 1999; (discussion 627–8).
- ²⁹Nachemson, A. The load on lumbar disks in different positions of the body. *Clin. Orthop. Relat. Res.* 45:107–122, 1966.
- ³⁰Nachemson, A. L. Disc pressure measurements. *Spine (Phila Pa 1976)* 6(1):93–97, 1981.
- ³¹Panjabi, M. M., J. J. Crisco, A. Vasavada, T. Oda, *et al.* Mechanical properties of the human cervical spine as shown by three-dimensional load-displacement curves. *Spine (Phila Pa 1976)* 26(24):2692–2700, 2001.
- ³²Pearcy, M. J., and S. B. Tibrewal. Lumbar intervertebral disc and ligament deformations measured in vivo. *Clin. Orthop. Relat. Res.* 191:281–286, 1984.
- ³³Setton, L. A., and J. Chen. Mechanobiology of the intervertebral disc and relevance to disc degeneration. *J. Bone Joint Surg. Am.* 88(Suppl 2):52–57, 2006.
- ³⁴Simpson, A. K., D. Biswas, J. W. Emerson, B. D. Lawrence, *et al.* Quantifying the effects of age, gender, degeneration, and adjacent level degeneration on cervical spine range of motion using multivariate analyses. *Spine (Phila Pa 1976)* 33(2):183–186, 2008.
- ³⁵Tashman, S., J. Princehorn, S. Pennatto, and W. Anderst. Bi-plane X-ray Imaging System. 2010, Google Patents.
- ³⁶Vergroesen, P. P., I. Kingma, K. S. Emanuel, R. J. Hoogendoorn, *et al.* Mechanics and biology in intervertebral disc degeneration: a vicious circle. *Osteoarthritis Cartilage* 23:1057–1070, 2015.
- ³⁷Wilke, H. J., P. Neef, M. Caimi, T. Hoogland, *et al.* New in vivo measurements of pressures in the intervertebral disc in daily life. *Spine (Phila Pa 1976)* 24(8):755–762, 1999.
- ³⁸Winter, D. A. *Biomechanics and Motor Control of Human Movement* (4th ed.). Hoboken: Wiley, 2009.
- ³⁹Womack, W., P. D. Leahy, V. V. Patel, and C. M. Puttlitz. Finite element modeling of kinematic and load transmission alterations due to cervical intervertebral disc replacement. *Spine (Phila Pa 1976)* 36(17):E1126–E1133, 2011.
- ⁴⁰Yukawa, Y., F. Kato, K. Suda, M. Yamagata, *et al.* Age-related changes in osseous anatomy, alignment, and range of motion of the cervical spine. Part I: radiographic data from over 1,200 asymptomatic subjects. *Eur. Spine J.* 21(8):1492–1498, 2012.